Induction of potent anti-tumor responses while eliminating systemic side effects via liposome-anchored combinatorial immunotherapy

Citation: Kwong, Brandon, Haipeng Liu, and Darrell J. Irvine. "Induction of Potent Anti-Tumor Responses While Eliminating Systemic Side Effects via Liposome-Anchored Combinatorial Immunotherapy." Biomaterials 32, no. 22 (August 2011): 5134–5147.

As Published: http://dx.doi.org/10.1016/j.biomaterials.2011.03.067

Publisher: Elsevier

Persistent URL: http://hdl.handle.net/1721.1/99424

Version: Author's final manuscript: final author's manuscript post peer review, without publisher's formatting or copy editing

Published as: *Biomaterials*. 2011 August ; 32(22): 5134–5147.

Induction of potent anti-tumor responses while eliminating systemic side effects via liposome-anchored combinatorial immunotherapy

Brandon Kwong[1], **Haipeng Liu**[1], and **Darrell J. Irvine**[1,2,3,4,5,*]

[1]Department of Biological Engineering, Massachusetts Institute of Technology, Cambridge, MA, USA

[2]Department of Material Science and Engineering, Massachusetts Institute of Technology, Cambridge, MA, USA

[3]Koch Institute for Integrative Cancer Research, Massachusetts Institute of Technology, Cambridge, MA, USA

[4]Ragon Institute of Massachusetts General Hospital, MIT and Harvard University, Boston, Massachusetts, USA

[5]Howard Hughes Medical Institute, Chevy Chase, Maryland, USA

Abstract

Immunostimulatory therapies that activate immune response pathways are of great interest for overcoming the immunosuppression present in advanced tumors. Agonistic anti-CD40 antibodies and CpG oligonucleotides have previously demonstrated potent, synergistic anti-tumor effects, but their clinical use even as monotherapies is hampered by dose-limiting inflammatory toxicity provoked upon systemic exposure. We hypothesized that by anchoring immuno-agonist compounds to lipid nanoparticles we could retain the bio-activity of therapeutics in the local tumor tissue and tumor-draining lymph node, but limit systemic exposure to these potent molecules. We prepared PEGylated liposomes bearing surface-conjugated anti-CD40 and CpG and assessed their therapeutic efficacy and systemic toxicity compared to soluble versions of the same immuno-agonists, injected intratumorally in the B16F10 murine model of melanoma. Anti-CD40/CpG-liposomes significantly inhibited tumor growth and induced a survival benefit similar to locally injected soluble anti-CD40+CpG. Biodistribution analyses following local delivery showed that the liposomal carriers successfully sequestered anti-CD40 and CpG *in vivo*, reducing leakage into systemic circulation while allowing draining to the tumor-proximal lymph node. Contrary to locally administered soluble immunotherapy, anti-CD40/CpG liposomes did not elicit significant increases in serum levels of ALT enzyme, systemic inflammatory cytokines, or overall weight loss, confirming that off-target inflammatory effects had been minimized. The development of a delivery strategy capable of inducing robust anti-tumor responses concurrent with minimal systemic side effects is crucial for the continued progress of potent immunotherapies toward widespread clinical translation.

*Correspondence should be addressed to D.J. Irvine. Department of Biological Engineering and Department of Materials Science and Engineering, Massachusetts Institute of Technology, 77 Mass. Ave., Cambridge, MA 02139, USA. Tel: 1-617-452-4174; Fax: 1-617-452-3293. djirvine@mit.edu.

Keywords

tumor immunotherapy; agonistic anti-CD40; CpG oligonucleotides; localized biodistribution; liposome delivery; reduced toxicity

1. Introduction

Tumors elicit tolerized immune responses against tumor-associated self-antigens while simultaneously inducing local immune suppression as a mechanism to avoid detection and elimination by the host immune system [1,2]. A potential therapeutic strategy to counter this immunosuppression is the use of non-cell-based therapies such as cytokines, immune receptor-targeting monoclonal antibodies, or Toll-like Receptor (TLR) agonists to break tumor-associated tolerance, blocking tumor-induced suppressive factors, or directly providing the costimulatory signals necessary to prime an anti-tumor immune [3-9]. However, these potent agents are also prone to eliciting serious side effects following systemic infusion [10-13]. Thus, the clinical effectiveness of many immuno-agonists has remained limited by the lack of a strategy to achieve therapeutic efficacy while avoiding excessive systemic exposure.

Anti-CD40 antibodies and CpG oligonucleotides are two immunostimulatory agents that exemplify this two-edged nature of immunotherapy. Agonists against CD40, a co-stimulatory receptor expressed on the surface of antigen-presenting cells (APCs), have been studied extensively for their ability to promote anti-tumor immunity. Triggering of CD40 signaling via anti-CD40 ligation provides strong activating signals to APCs, endowing them with the capacity to prime strong anti-tumor cytotoxic T-cell responses [14-16]. Pre-clinical studies have shown the efficacy of anti-CD40 therapy against a wide variety of tumor models, either as a monotherapy [17-19], in combination with chemotherapy [20], or in combination with other immunostimulants such as interleukin (IL)-2 [21,22]. These promising results led to the use of anti-CD40 therapy in phase I clinical trials for human patients suffering from non-Hodgkins lymphoma, multiple myeloma, and other solid malignancies [23-26]. However, despite achieving moderate levels of therapeutic efficacy, the maximum tolerated dose for human therapy has been limited due to inflammatory effects in off-target organs [23-25]. Intravenous infusion of anti-CD40 results in widespread systemic exposure to the immunoagonist, leading to symptoms of cytokine release syndrome (fever, headaches, nausea, chills), noninfectious ocular inflammation, elevated hepatic enzymes (indicative of liver damage), and hematologic toxicities including T-cell depletion. Severe off-target inflammatory effects in the liver, lungs, and gut have previously been observed in mice as well, including similar evidence of systemic cytokine release [27-30]. Although the aforementioned side effects were mostly transient in nature, two recent studies in mice unexpectedly observed long-term immuno-suppression following anti-CD40 therapy as well, possibly relating to the activation-induced apoptosis of $CD4^+$ or $CD8^+$ T-cells [31-32].

CpG oligonucleotides, ligands for Toll-like receptor (TLR) 9 expressed by APCs, represent another class of potent immunostimulatory factors. Stimulation of the TLR9 receptor directs APCs towards priming potent, T_H1-dominated T-cell responses, by increasing the production of pro-inflammatory cytokines and the presentation of co-stimulatory molecules to T cells [33]. Like anti-CD40, CpG therapy has been tested against a wide variety of tumor models in mice, and has consistently been shown to promote tumor inhibition or regression [6,34-36]. Furthermore, the combination of CD40 agonists and TLR ligands can synergize to stimulate highly potent anti-tumor responses *in vivo* [37-40]. However, recent studies have also suggested that systemic over-exposure to CpG can have potentially dangerous side

effects, including lymphoid follicle destruction [41] and the suppression of adaptive T-cell immunity via indoleamine 2,3-dioxygenase (IDO) induction in the spleen [42,43]. Thus, both anti-CD40 and CpG show substantial anti-tumor potency concurrent with issues of systemic toxicity.

In light of the dangers of systemic immunostimulatory therapy, intratumoral or peritumoral treatments have been tested in an attempt to reduce the level of systemic exposure to potent immuno-agonists. In the clinical setting, local immunotherapy has so far been proposed primarily for the treatment of unresectable tumors or for post-surgical adjuvant therapy to prevent local recurrence [44-47]. However, pre-clinical studies in animal models have also shown that the generation of a local anti-tumor immune response can drive systemic/distal tumor inhibition, via the induction of tumor antigen-specific immune memory. The priming of an adaptive anti-tumor immune response is highly attractive since it could enable immunological targeting of unknown tumor metastases or disseminated malignancies, following locally delivered immunotherapy at a known tumor site. Local therapies applied at a single tumor site using anti-CD40 [18], CpG [36], target antibody-cytokine (IL-2) fusion proteins [48], or other immunostimulants [8,49-52] have successfully inhibited the growth of distal untreated tumors. Furthermore, the intratumoral injection of CpG has recently been tested in a phase I clinical trial against B-cell lymphoma in humans, and some patients exhibited anti-lymphoma clinical responses at distant, untreated tumor sites [53].

Despite such therapeutic benefits, pre-clinical and clinical studies have established that the local injection of soluble agonists [54-57] or controlled release of drugs from a local injection site [58-60] does not necessarily prevent such agonists from entering the systemic circulation and dispersing to distal organs. This could occur either by drainage through lymphatics to the thoracic duct or via direct entry into the bloodstream from leaky tumor vessels. In mice, subcutaneous or intratumoral administrations of the immunotherapeutic cytokines IL-2 [56] or IL-12/GM-CSF [59] resulted in rapid clearance from the local injection site and detection in other peripheral organs within minutes after injection. Similarly, in human patients, high circulating levels of IL-12 [61] or IL-2 [54] were observed within 30 minutes or 3 hours (respectively) after intratumoral/subcutaneous injection. Such observations have necessitated the use of isolated organ perfusion in order to withstand the systemic toxicity of some local recombinant cytokine therapies [62,63]. As a result, the maximum tolerated dose in local immunotherapy may still be restricted by the need to limit undesired widespread exposure and off-target inflammatory symptoms. With this motivation, we sought to develop a biomaterial-based delivery strategy for immunostimulatory factors that could physically retain injected therapeutics at a local tumor site and limit their tissue drainage, while retaining their potent therapeutic efficacy in activating an anti-tumor immune response.

In order to accomplish this, we developed a strategy to couple anti-CD40 and CpG to the surface of PEGylated unilamellar liposomes, for simultaneous co-delivery. We hypothesized that anchoring these molecules to liposomal carriers with a more confined bio-distribution following intratumoral injection would enhance the local retention of these ligands while maintaining their bioactivity. Intratumoral injections of anti-CD40/CpG combination liposomes were performed in established subcutaneous B16F10 tumors in order to investigate whether immunostimulatory effects could be limited to the treated tumor and the tumor-proximal lymph node, thereby driving tumor inhibition while avoiding the inflammatory side effects that result from systemic exposure to these agonists.

2. Materials and Methods

2.1. Materials

Monoclonal anti-CD40 (clone FGK4.5, rat IgG2a) was purchased from Bio X Cell (West Lebanon, NH). Cholesterol, dithiothreitol (DTT), and Tween 20 were obtained from Sigma-Aldrich (St. Louis, MO). Zeba desalting columns were from Pierce (Thermo Fisher Scientific, Rockford, IL). Phospholipids dioleoylphosphocholine (DOPC), polyethylene glycol (PEG)2000-distearoylphosphoethanolamine (DSPE), maleimide-PEG2000-DSPE, and rhodamine-dioleolyphosphoethanolamine (DOPE) were purchased from Avanti Polar Lipids (Alabaster, AL). Fluorescein amidite (FAM)-labeled CpG oligonucleotide (sequence 1826, with phosphorothioate backbone) and FAM-labeled CpG-PEG-lipid conjugate were synthesized in-house as previously described [64]. DNA synthesis reagents were purchased from Glen Research (Sterling, VA) or ChemGenes (Wilmington, MA). Anti-mouse CD45 (clone 30-F11), anti-mouse F4/80 (BM8), anti-mouse CD11c (N418), and polyclonal anti-rat IgG-HRP were obtained from eBioscience (San Diego, CA). Secondary anti-rat IgG was purchased from Jackson ImmunoResearch Labs (West Grove, PA). TNF-alpha and IL-6 ELISA kits were purchased from R&D Systems (Minneapolis, MN). Purified anti-human IgG and recombinant mouse CD40/human Fc fusion protein, for the sandwich ELISA of anti-CD40, were also purchased from R&D Systems.

2.2. Animals and cells

Animals were cared for in the USDA-inspected MIT Animal Facility under federal, state, local and NIH guidelines for animal care. C57BL/6 female mice were purchased from the Jackson Laboratory. For tumor experiments, all mice were inoculated between 6-8 weeks of age. B16F10 melanoma cells were purchased from American Type Culture Collection, and certified to be mycoplasma-free prior to inoculation into animals.

2.3. Synthesis of liposome-anchored anti-CD40 and CpG

Liposomes were synthesized with a composition of cholesterol/DOPC/maleimide-PEG-DSPE/PEG-DSPE 35/50/5/10 by mol%; 0.5 mol% of fluorescent rhodamine-labeled DOPE was also incorporated for biodistribution experiments (histology and flow cytometry). Lipids were vacuum-dried, rehydrated in PBS at 15 μmol/ml, and sonicated for 4 min (alternating 5-7 Watts) using a Misonix probe-tip sonicator (Qsonica, Newtown, CT) to form unilamellar liposomes. Anti-CD40 with exposed free hinge-region thiols was prepared by mixing anti-CD40 (12-15mg/ml) with a 25X molar excess of DTT for 20 min at 25°C in the presence of 10mM EDTA in PBS. The mildly reduced anti-CD40 was passed through a desalting column to remove DTT, and then immediately mixed with maleimide-functionalized liposomes at a ratio of 3 mg Ab:1 μmol liposomes for covalent coupling in the presence of 10 mM EDTA. The maleimide-thiol reaction was allowed to proceed for at least 10 hr at 25°C, followed by centrifugation of the resulting aggregated liposomes and multiple washes with PBS, to remove unbound antibody. Prior to use, anti-CD40-liposomes were syringe-extruded 25X through 100nm polycarbonate filter membranes (Avanti Polar Lipids).

Lipid-conjugated CpG was prepared as previously described [64]. Briefly, CpG oligonucleotides were synthesized using the ABI 394 DNA synthesizer (Applied Biosystems, Carlsbad, CA), and lipid phosphoramidite containing a 24-unit PEG spacer was synthesized as previously described [64]. Lipid phosphoramidite was then dissolved in dichloromethane and coupled to CpG DNA for 15min, using the DNA synthesizer. Following synthesis, CpG and CpG-PEG-lipid conjugates were purified by reverse phase HPLC. To create combination liposomes simultaneously bearing anti-CD40 + CpG, a post-insertion approach [65] was used to insert the purified CpG-lipid conjugate onto the surface of anti-CD40-conjugated liposomes: ~3nmol CpG-lipid was mixed with previously prepared

anti-CD40-liposomes (1μmol) for 2hr at 25°C. The resulting combination liposomes were again centrifuged and washed multiple times with PBS, to remove unimer or micellar CpG-lipid, then syringe-extruded 25X through 200nm polycarbonate filter membranes (Avanti). Final liposome size distributions were characterized by dynamic light scattering (Brookhaven 90Plus Particle Size Analyzer, Worcestershire, UK). All liposomes were stored in PBS at 4°C until use.

2.4. Quantitation of anti-CD40 and CpG coupling to liposomes

Bioactive anti-CD40 conjugated to liposomes was quantified by a functional ELISA assay. Anti-CD40 liposomes were first mixed with PBS containing 0.5% Tween 20 surfactant to solubilize the lipids. Standard 96-well plates were coated with 2 μg/ml of goat anti-human IgG antibody, followed by the addition of 100 ng/ml recombinant mouse CD40/human Fc fusion protein. Use of recombinant CD40 as the capture agent for lipid-anchored anti-CD40 ensured that only bioactive anti-CD40 still capable of binding its target receptor would be quantitated. 200 ng/ml of HRP-conjugated goat anti-rat IgG was then added as the detection antibody, followed by an HRP-sensitive colorimetric substrate (R&D Systems). CpG and CpG-lipid were both tracked using a fluorescent FAM label on the 3' end, and fluorescent measurements were taken at ex/em wavelengths of 480/520nm.

2.5. In vitro release of anti-CD40 and CpG from liposomes

To measure the *in vitro* release of anti-CD40 or CpG-lipid from combination liposomes, dialysis cassettes (1ml capacity) with a 300kD MWCO membrane were used (Float-a-lyzer G2, Spectrum Labs, Rancho Dominguez, CA). 400μl samples were dialyzed against 20ml PBS containing 10% fetal calf serum, with gentle agitation, at 37°C. Samples and dialysis buffers were collected at each indicated timepoint; anti-CD40 was measured by sandwich ELISA and CpG was measured by its fluorescent label FAM. All samples were mixed with 0.5% Tween 20 to disrupt intact liposomes prior to the anti-CD40 ELISA.

2.6. Tumor inoculation and tumor therapy experiments

For *in vivo* tumor experiments, C57BL/6 mice were anaesthetized and inoculated subcutaneously on the right hind flank with 5×10^4 B16F10 cells in Hank's Balanced Salt Solution (HBSS). Tumors were allowed to establish for 8 days before the start of therapy, by which time they had reached an average area of ~12 mm^2. Tumor sizes were measured every 1-2 days by electronic caliper and calculated as the product of 2 orthogonal diameters ($D_1 \times D_2$). For anti-tumor therapy experiments, mice received intra-tumoral injections on days 8, 10, 12, and 14 of PBS, soluble anti-CD40 only, anti-CD40-liposomes, soluble anti-CD40 + CpG, or combination liposomes, diluted in 150 μl of PBS. Each dose, whether in soluble or liposomal form, consisted of 40 μg of anti-CD40, with or without 20 μg of CpG. Body mass of treated mice was measured daily, beginning on day 7 post-tumor inoculation, using an electronic scale. Serum was collected from mice at the indicated time points via retro-orbital bleeding, for the measurement of circulating inflammatory markers. Mice were euthanized when tumor areas exceeded 100 mm^2, per institutional guidelines.

2.7. Serum measurements of systemic side effects

Blood was collected from mice at the indicated time points and centrifuged to remove the cellular fraction. Circulating serum levels of TNF-alpha and IL-6 were measured by ELISA detection kits (R&D Systems), according to the manufacturer's instructions. The serum level of free anti-CD40 was measured by sandwich ELISA using recombinant CD40 receptor (described in section 2.4), and serum CpG was detected via its fluorescent FAM label (ex/em at 480/520nm). Serum levels of the hepatic enzyme ALT (alanine transaminase) were

determined using a standard biochemical assay (Infinity ALT reagent kit, Thermo Fisher), according to the manufacturer's instructions.

2.8. Histological and flow cytometric analysis

For biodistribution experiments, a single intratumoral injection of soluble or liposomal formulations was given at a dose of 40 μg anti-CD40 ± 20 μg CpG between days 8-10 post-inoculation when tumors were at a size of 12-15 mm^2, and mice were euthanized 24hr or 48hr later. Tumors, tumor-proximal or distal lymph nodes, and spleens were harvested and either immediately snap-frozen using liquid nitrogen (for cryosectioning) or digested with 100μg/ml Liberase Blendzyme III (Roche Applied Sciences, Indianapolis, IN) for 15min at 37°C, followed by mechanical dissoctiation and rinsing through 40 μm nylon mesh cell strainers to obtain cell suspensions. Cryosections were sliced at a thickness of 7μm, and imaged directly without any further processing for the optimal detection of fluorescent FAM-labeled CpG, FAM-labeled CpG-lipid, and rhodamine-labeled liposomes. All brightfield and fluorescent images were taken using a Zeiss LSM 510 confocal microscope, and processed using Zeiss LSM 510 Image Browser. For secondary immunostaining against anti-CD40, cryosections were acetone-fixed and stained using a DyLight649-labeled anti-rat IgG, with minimal cross-reactivity against mouse IgG (Jackson Immuno). After washing, stained cryosections were mounted and covered using VectaShield HardSet mounting medium with DAPI (Vector Laboratories, Burlingame, CA). For flow cytometry analysis, recovered cells were re-suspended in PBS + 1% BSA and stained with fluorescent antibodies against CD45, CD11c, and F4/80, for 30-40min on ice. Flow cytometry was performed on an LSRII cytometer (BD Biosciences) and data was processed using FlowJo software (Tree Star, Ashland, OR). Cellular events were gated based on forward and side scatter, and tumor-infiltrating leukocytes were gated from other cell populations based on CD45 expression.

2.9. Statistical analysis

Data are shown as mean ± SEM, unless indicated otherwise. Comparisons of Kaplan-Meier survival curves were performed using a log-rank test. For all other data, comparisons of two experimental groups were performed using two-tailed unpaired t-tests unless indicated otherwise. Statistical analysis was performed using GraphPad Prism software.

3. Results

3.1. Synthesis and characterization of liposomes for the combined delivery of immunostimulatory *anti-CD40 and CpG*

Immunotherapy using soluble immuno-agonists can be effective but is known to have systemic toxicity even following local administration [54,55,62]. To test whether nanoparticle anchoring could restrict the dissemination of conjugated immunostimulatory ligands following local injection while maintaining their ability to effectively stimulate target cell populations, we began by preparing immunoliposomes for anti-CD40 delivery into tumors. Monoclonal agonistic anti-CD40 was mildly reduced to selectively cleave disulfides in the hinge region of the antibody [66], and then mixed with maleimide-functionalized small unilamellar vesicles (SUVs) (cholesterol:DOPC:PEG-DSPE:maleimide-PEG-DSPE in a 35:50:10:5 mol% ratio) with a mean diameter of 80 nm (± 15nm std. dev.) (Fig. 1A). Aggregation of liposomes occurred during the coupling reaction, consistent with the availability of multiple thiol groups per antibody, which could mediate crosslinking between liposomes. However, because the lipids themselves can readily reorganize during processing, we used this crosslinking phenomenon to quickly purify the reaction components: The aggregated liposomes were pelleted by centrifugation, washed to remove unbound antibody, then re-sized by membrane extrusion (Fig. 1A) to obtain

homogeneous Ab-conjugated vesicles with a mean diameter of approximately 100 nm and a standard deviation of 14 nm (Fig. 1B). Quantitation of coupled anti-CD40 was performed by sandwich ELISA analysis of liposomes lysed by Tween 20 surfactant, using recombinant CD40 as the capture ligand to measure the amount of bioactive antibody linked to the vesicles. Anti-CD40 binding to the liposomes required the presence of maleimide-functionalized lipid, and the amount of bioactive Ab conjugated was only weakly influenced by the quantity of maleimide-PEG-lipid included in the vesicle composition (Supplementary Fig. 1). We thus chose to use liposomes with 5 mol% mal-PEG-DSPE for further studies, which consistently gave conjugations of ~55 μg bioactive conjugated anti-CD40 per mg lipid (Supplementary Fig. 1).

To co-incorporate anchored CpG oligonucleotides into anti-CD40-bearing immunoliposomes, we employed a synthetic CpG-PEG-lipid conjugate recently developed in our lab (Fig. 1A) [64]. When suspended alone in aqueous buffer, the CpG-PEG-lipid conjugate self-assembled into stable micelles, but mixing of these oligo-micelles with anti-CD40-liposomes led to rapid spontaneous insertion of the lipophilic tails of the CpG conjugate into the liposomal membranes. Anti-CD40 was conjugated to liposomes as described above, and following washing to remove unbound antibody, the aggregated liposomes were mixed with lipid-CpG (Fig. 1A). After washing again to remove unbound CpG, the anti-CD40/CpG-coupled liposomes were membrane-extruded to a mean diameter of approximately 150 nm, with a std. dev. of 18 nm (Fig. 1B). Mixing fluorescently-tagged CpG-lipid (130 μg/ml) with anti-CD40-liposomes (14.4 mg lipid/mL) gave CpG insertion with ~90% efficiency, resulting in 20 ± 2.2 μg CpG oligonucleotides (~3 nmol) per total mg liposomes. The high efficiency of CpG-lipid association with liposomes and high level of CpG loading per lipid mass contrasted with the low efficiency of soluble non-lipidated CpG entrapment we could achieve by traditional liposomal encapsulation in PEGylated liposomes, where only 2 μg of CpG was encapsulated per mg lipid. The mean sizes of anti-CD40-liposomes or combination liposomes were stable for at least 7 days in storage at 4°C (data not shown).

To test the stability of anti-CD40 and CpG association with PEGylated liposomes, the release of the immunostimulatory ligands from vesicles was measured *in vitro* in the presence of serum: combination liposomes carrying anti-CD40 and CpG were dialyzed (300kD MWCO membrane) against PBS pH 7.4 containing 10% fetal calf serum at 37°C, and release of the ligands into the dialysis buffer was monitored over time. Soluble anti-CD40 and CpG both diffused freely through the membrane with substantial release from the dialysis cassette in <5 hr (Fig. 2A-B). By contrast, PEG-DSPE-anchored anti-CD40 effectively tethered the antibody to the liposome surfaces, with <10% of the initial loading released over 7 days (Fig. 2A). After 7 days, the liposomes were disrupted by adding 0.5% Tween 20 surfactant, and >90% of the coupled anti-CD40 was immediately recovered. CpG-lipid inserted into combination liposomes was retained by the vesicles less efficiently; nearly 80% of the oligo was released by 24 hr and release was complete by ~7 days (Fig. 2B). CpG release may reflect the ability of oligo-lipids to self-assemble favorably into highly stable micelles in aqueous buffers [64]. Gel electrophoresis of released samples confirmed that the fluorescent measurements of labeled CpG represented fully intact FAM-labeled CpG-lipid, with only a low level of degradation of these phosphorotioate backbone-stabilized oligos (or cleavage of the FAM label) by serum nucleases over 24 hr (data not shown). Thus, the vesicles efficiently retain anti-CD40 but release CpG over approximately one week under strong sink conditions. Combination liposomes stored in PBS at 4°C showed negligible loss of either anti-CD40 or CpG over at least 2 weeks (data not shown).

3.2. Anti-tumor efficacy and systemic toxicity following intratumoral injection of anti-CD40-displaying liposomes

Many previous preclinical studies have demonstrated that anti-CD40 monotherapy can lead to inhibition of tumor growth or even complete tumor regression in some animal models [11,15-18]. We thus initially tested the efficacy of anti-CD40-liposomes alone, without CpG, in the aggressive, poorly immunogenic B16F10 transplanted melanoma model [19]. We first confirmed that anti-CD40-liposomes did not directly exert cytotoxic effects on B16 tumor cells during *in vitro* culture, and that tumor cells exhibited minimal non-specific binding of immunoliposomes, consistent with the absence of CD40 surface expression on B16F10 cells (Supplementary Fig. 2 and data not shown). For *in vivo* experiments, C57BL/6 mice were inoculated s.c. in the flank with B16F10 tumor cells, which were allowed to establish into a solid tumor for 8 days, to a mean size of ~12 mm^2. Starting on day 8, mice were given 4 intratumoral injections of anti-CD40-liposomes or soluble anti-CD40, every other day, at an equivalent dose of 40 μg antibody per injection. While locally administered soluble anti-CD40 strongly inhibited B16 tumor growth, anti-CD40-liposomes slowed tumor growth only ~50% as effectively as the soluble antibody (Fig. 3A-B).

In parallel with measuring the anti-tumor activity of these two different treatments, we also assessed systemic toxicity associated with each therapy. Even when administered locally, soluble anti-CD40 caused a substantial weight loss in treated mice for several days following the initiation of therapy, which was statistically significant (versus PBS-injected controls) on days 2-6 after the start of therapy. The weight loss peaked at ~10% on day 3, comparable to the loss experienced by mice in an inflammatory lipopolysaccharide (LPS)-induced acute phase response [67,68]. This result is consistent with the expectation that soluble anti-CD40 can drain rapidly from the injection site, enter the systemic circulation, and cause widespread inflammatory effects. The transient nature of the systemic response to soluble anti-CD40 has been previously observed and may reflect systemic tolerization to the antibody's effects on repeated treatment [27,39]. In contrast, treatment with anti-CD40-liposomes did not cause significant weight loss relative to PBS-treated controls at any time point (Fig. 3C). Measurements of circulating serum levels of pro-inflammatory cytokines such as IL-6 provided a further indication of systemic inflammation in response to local soluble immunostimulant therapy (Fig. 3D). Intratumorally injected anti-CD40 caused a dramatic increase in serum IL-6 within 24hr, but anti-CD40-displaying liposomes induced a barely detectable ($p=0.11$, n.s.) increase in serum cytokine levels over control mice. Similar trends were observed with serum levels of the inflammatory cytokine tumor necrosis factor-alpha (TNF-α), and alanine transaminase (ALT) enzyme, a standard clinical measure of hepatic inflammatory damage (data not shown). While these results confirmed the potential benefits of liposomal anchoring for eliminating systemic side effects, liposomal anchoring clearly inhibited the anti-tumor efficacy of anti-CD40 monotherapy.

3.3. Therapeutic efficacy and systemic toxicity of combination anti-CD40/CpG liposomes

Combination therapies of anti-CD40 mixed with TLR agonists such as CpG oligonucleotides have previously been shown to provide substantially enhanced anti-tumor immune responses compared to anti-CD40 monotherapy [38-40]. We reasoned that the enhanced potency of anti-CD40 + CpG signaling combined with the controlled release of CpG-lipid from liposomes (as indicated by our *in vitro* data) might allow the liposome-delivered combination therapy to achieve potency comparable to soluble anti-CD40+CpG therapy, while still avoiding systemic inflammation that might be augmented by the addition of soluble CpG. We thus proceeded to test the anti-tumor efficacy of soluble or liposomal combination anti-CD40/CpG in the B16 model. As before, mice received 4 intratumoral injections (given every other day starting day 8 post tumor cell inoculation) of either soluble anti-CD40 alone, soluble anti-CD40 mixed with CpG, or anti-CD40/CpG liposomes, at

equivalent doses of 40 μg anti-CD40 and 20 μg CpG per injection. As shown in Fig. 4A, 3/9 mice treated with soluble anti-CD40+CpG exhibited "complete responses", defined as apparent cures of the animals and lack of tumor progression or new tumor nodule formation over 45 days. The remaining mice showed a delay in tumor growth compared to untreated animals but eventually all succumbed (Fig. 4B); we quantified this delay in tumor growth as a time to progression (time to tripling of initial tumor size from the start of therapy) (Fig. 4C). Such a mixture of complete and partial responses to immunotherapy has previously been reported and has been correlated with the tumor size at the start of treatment [8]. In the current study, however, the initial tumor burden of the three mice showing the strongest anti-tumor responses was only slightly smaller than that of the other six mice (mean 9.3 ± 0.7 mm^2 vs. 12 ± 2 mm^2, n.s.). The combination of soluble CpG with soluble anti-CD40 provided only a modest enhancement over soluble anti-CD40 alone, which induced 2/8 complete responses and showed a slightly longer time to progression for the remaining tumors (Fig. 4A-C). No significant difference in survival benefit was observed between either regimen of soluble therapy (Fig. 4B, p=0.33, n.s. by log-rank test).

In comparison, liposomal anti-CD40/CpG elicited no complete responses (0/9), but instead showed a significant increase in the time to progression for partial responders compared to the equivalent soluble therapy (p = 0.04), from a mean of 27.8 ± 1.4 days for soluble treatment to 33.4 ± 1.8 days for liposomal anti-CD40/CpG (Fig. 4A-C). Anti-CD40/CpG liposome therapy significantly prolonged the survival of tumor-bearing mice compared to PBS-treated controls (Fig. 4B, p<0.0001 by log-rank test), and induced a mean survival benefit comparable to both soluble immunotherapy regimens (p>0.05, not significant). Furthermore, combinatorial liposome therapy demonstrated a substantial increase in potency over liposomal anti-CD40 alone (Figs. 3B vs. 4A), suggesting a synergistic effect in the particle-mediated co-delivery of both immuno-stimulants. Thus, though liposomal therapy showed the loss of a minority of complete responses seen with soluble immunostimulatory ligands, the majority of animals (partial responders in all groups) actually exhibited longer times to progression following liposomal therapy compared to the soluble treatment regimens.

To determine whether the therapeutic effects of anti-CD40/CpG liposomes was still achieved with minimized systemic side effects, overall weight loss and circulating serum inflammatory markers were monitored following locally-administered therapy. The addition of soluble CpG to soluble anti-CD40 intratumoral therapy greatly exacerbated the weight loss of animals through the entire course of treatment (Fig. 5A vs. Fig. 3C), showing statistically significant differences versus PBS-treated animals from day 9 through day 16 (p≤0.04). In contrast, anti-CD40/CpG-liposomes showed a mild, transient effect that reached statistical significance only on day 10 (mean 4% weight loss at this time point, p=0.04) (Fig. 5A). Serum levels of hepatic ALT enzyme were significantly elevated in mice at 24 hr after the first injection of soluble anti-CD40 + CpG, indicative of inflammatory hepatic damage (Fig. 5B), while mice treated with anti-CD40/CpG liposomes showed a barely detectable increase above background levels that did not reach significance (p=0.07, n.s.). Similarly, serum levels of the pro-inflammatory cytokines IL-6 and TNF-α were greatly increased in mice that received soluble anti-CD40/CpG, but not in mice that received liposome-anchored agonists (Figs. 5C-D). Taken together, these data demonstrate that dual-agonist immunotherapy employing liposomal delivery was capable of stimulating a potent local anti-tumor immune response, without inducing the systemic toxicity elicited by an equivalent dose of locally-administered soluble agonists.

3.4. Biodistribution of liposome-anchored anti-CD40 and CpG

To determine whether the lack of systemic inflammation following liposome-anchored αCD40/CpG delivery was achieved as a result of lowered systemic exposure to these agents,

we collected blood serum at various time points following intratumoral injections. Consistent with the *in vitro* release data, negligible levels of anti-CD40 could be detected in serum at 6 or 24 hr after local liposome-anchored αCD40/CpG therapy (Fig. 6A, or later times, not shown), indicating that lipid anchoring effectively prevented dissemination of the antibody to the systemic circulation. In contrast, locally-administered soluble anti-CD40+CpG or anti-CD40 alone resulted in high levels of circulating antibody within 6 hr post-injection (Fig. 6A and data not shown). The release of liposome-inserted CpG-lipid from combination liposomes occurred much more rapidly than the release of lipid-anchored anti-CD40 *in vitro* (Fig. 2), so a similar trend was expected *in vivo*. Fig. 6B shows that fluorescently-labeled CpG from combination liposome delivery could be detected in serum at 5 hr following intra-tumoral injection, and also remains present at a measurable level in serum up to 20 hr post-injection. However, the level of circulating CpG following liposomal delivery was approximately half that attained following intratumoral soluble anti-CD40+CpG therapy at both time points ($p=0.0008$ and $p=0.002$, respectively, Fig. 6B). Thus, liposome-anchored CpG delivery lowered the systemic exposure to this agent as well.

Low levels of anti-CD40 and CpG in the serum following liposomal delivery could either reflect preferential retention of the nanoparticle-anchored agonists in the tumor site/tumor draining lymph nodes or more rapid clearance/degradation of the particle-delivered agonists. We thus performed histological analysis on cryosections of tumors and tumor-draining lymph nodes, to directly visualize the local retention and proximal draining of intratumorally-injected immunostimulatory ligands. Established B16 tumors were given a single intratumoral injection of PBS, soluble unlabeled anti-CD40 + FAM-labeled CpG, or rhodamine-tagged liposomes conjugated with anti-CD40 and FAM-labeled CpG-lipid. Fig. 7A shows representative cryosections of tumors excised at 48hr following soluble or combination liposome therapy (refer to Supplementary Fig. 3A for PBS controls). Liposomes (red) were retained at a high level at the tumor for over 48 hr post-injection, while secondary anti-rat IgG staining (yellow) against anti-CD40 co-localized closely with the liposomes, confirming that anti-CD40 remained coupled to the liposome carrier *in vivo*. FAM-labeled CpG-lipid (green) was also highly retained at the tumor site for at least 48hr following liposomal delivery, but was more dispersed through the local dermal and subcutaneous tissue. This was consistent with the release of CpG-lipid from liposomes that had been observed in the presence of serum *in vitro*. Tumors that received soluble anti-CD40+CpG therapy also showed significant levels of CpG remaining in the tumor site at 24 and 48 hr, consistent with earlier reports of the nonspecific interactions of phosphorothioate-backbone CpG with tissue matrix proteins [69,70]. However, significantly lower amounts of anti-CD40 remained within the tumor mass following soluble therapy, (Fig. 7A), indicating rapid draining away from the injection site.

The initiation of antigen-specific anti-tumor responses requires the interactions of activated APCs and T-cells in the tumor-proximal lymph node (LN). Since this is also the collection site for lymphatic draining from the tumor, we examined whether anti-CD40 and CpG reached the tumor-proximal LN following soluble or liposomal delivery. At 24 hr following treatment with anti-CD40/CpG liposomes, a low level of rhodamine-labeled lipid (Figure 7B, red) was observed, primarily at the subcapsular and intermediate sinus areas, co-localized with secondary staining for anti-CD40 (yellow). As with the tumor cryosections, FAM-labeled CpG-lipid (green) appeared to be distributed in a more dispersed pattern than the liposomes/anti-CD40. By 48hr, fluorescent signals from rhodamine-liposomes, FAM-CpG, or secondary anti-CD40 staining in the tumor-proximal LN of liposome-treated mice were greatly diminished, though still detectable above PBS-treated background levels (Supplementary Fig. 3B and data not shown). By comparison, mice that received soluble anti-CD40+CpG therapy showed surprisingly low levels of CpG in the tumor-draining LN, at both 24hr (Fig. 7B) and 48hr (not shown). Soluble anti-CD40, however, was readily

detected in a diffuse pattern in the tumor-proximal LN at both timepoints, consistent with the tumor-site and serum observations that locally-administered soluble anti-CD40 drains rapidly from the injection site into lymphatic or systemic circulation.

Given the persistence of liposomal anti-CD40/CpG in the tumors and draining lymph node, and the observed colocalization of anti-CD40 with liposomes but dispersion of CpG-lipid, we used flow cytometry to separately trace the binding/uptake of CpG and liposomes by cells at these sites following local therapy. Established B16 tumors were injected once intratumorally with either PBS, soluble anti-CD40 + FAM-labeled CpG, or combination liposomes carrying anti-CD40/FAM-labeled CpG-lipid/fluorescent rhodamine-lipid. At 24 or 48 hr post-injection, the tumor tissues, distal and tumor-proximal lymph nodes, and spleens were harvested and processed into cell suspensions for analysis. Cells were gated on CD45 expression (common leukocyte marker), CD11c (marker for dendritic cells), and F4/80 (macrophages), since these antigen-presenting cells express both the CD40 receptor and the TLR9 receptor for CpG, and represent primary targets of this immunotherapy. Figure 8A shows representative flow cytometry histograms of excised tumor samples at 48 hr post-injection, illustrating that the majority of tumor-infiltrating DCs ($CD45^+CD11c^+$) and macrophages ($CD45^+F4/80^+$) were positive for rhodamine-labeled liposomes (with their coupled anti-CD40 cargo) and FAM-labeled CpG. As summarized in Figure 8B, this high level of uptake by tumor-infiltrating APCs was consistently observed at both 24 and 48 hr post-injection, indicating that liposomally delivered anti-CD40/CpG therapy had reached its intended targets for local immuno-modulation.

Consistent with the histological data, flow cytometry analysis of proximal and distal lymphoid organs following intratumoral injection confirmed that a small fraction of leukocytes in the tumor-proximal LN took up liposomes (Fig. 8C) and ~10% of these cells took up CpG-lipid (Fig. 8D). As expected, barely detectable levels of either component were observed in spleens or contralateral lymph nodes, consistent with the elimination of systemic toxicity via liposomal coupling and local retention. $CD11c^+$ dendritic cells and $F4/80^+$ macrophages in the tumor-draining LN both took up rhodamine-labeled liposomes and FAM-labeled CpG by 24hr post-injection (Fig. 8E), suggesting the successful delivery to APCs in the draining LN, and fluorescent CpG could still be detected at 48 hr post-injection. In addition, higher overall levels of FAM-labeled CpG were observed in the proximal LN following combination liposome delivery than following soluble delivery, as quantified by mean fluorescent intensity in cells at both time points (Fig. 8F). This suggests that the CpG-PEG-lipid conjugate achieved enhanced draining to the proximal lymph node compared to free soluble CpG.

4. Discussion

The clinical usage of immunotherapy for tumor treatment has been hindered by evidence of dose-limiting toxicities, observed in pre-clinical animal studies and early human clinical trials [12,13,23-26]. Finding an appropriate dosing regimen that can balance between stimulating an anti-tumor immune response and avoiding off-target inflammatory effects has proven to be challenging for a number of immunomodulatory agonists. For example, the co-administration of interleukin-12 (IL-12) and IL-18 therapy causes a fatal inflammatory response in mice [12], while the systemic toxicity of recombinant IL-2 therapy at high doses in humans is well established [10]. Immuno-agonistic antibodies that remain in the process of clinical testing include anti-CD40 and anti-CTLA-4, both of which have demonstrated anti-tumor efficacy simultaneous with dose-limiting systemic side effects [13,23-25]. Nevertheless, the therapeutic potency of such immunotherapeutics has been well established, suggesting that developing a strategy for the restricted delivery of these compounds could substantially improve their prospects for clinical translation.

Other previous studies have attempted to address the issue of minimizing systemic side effects of immunostimulatory therapy. In one recent study, Ahonen et al [39] found paradoxically that the hepatotoxic effects of intravenous anti-CD40 therapy could be greatly reduced or even eliminated by the systemic co-adminstration of a TLR7 agonist. The authors were not able to determine specific cellular or molecular mechanisms by which the combined therapy could result in reduced toxicity. Based on our own data, this reduction of toxicity is not universal to the combination of all TLR agonists with anti-CD40 therapy, since the addition of CpG (TLR9 agonist) to soluble anti-CD40 therapy in the current study significantly increased symptoms of systemic inflammation (Figs. 3, 5), rather than decreasing them. The use of targeting motifs to enhance the specific localization of immunostimulatory ligands at tumor sites represents another possible strategy for reducing the off-target inflammatory effects of systemically administered immunotherapy. In two separate studies, Hamzah et al described the use of fusion peptide-targeted anti-CD40 + IL-2 [22], or surface peptide-targeted liposomes encapsulating CpG [74]. Although both methods succeeded in increasing the localization of therapy to the tumor site and greatly improved the anti-tumor response relative to non-targeted therapy, neither strategy was able to eliminate systemic exposure to the immuno-stimulatory agonists. Targeted delivery of anti-CD40 + IL-2 still resulted in elevated serum levels of hepatic ALT enzyme and the inflammatory cytokine TNF-α, while targeted delivery of CpG-liposomes could not prevent non-specific scavenging by the reticulo-endothelial system (RES), as indicated by substantial particle uptake in the spleen. Similarly, Johnson et al [48] studied the intravenous administration of a tumor antigen-targeted antibody-IL-2 fusion protein, and found that less than 5% of the injected dose actually reached the tumor following i.v. delivery, confirming that the use of tumor-specific antibody targeting is not sufficient to abrogate systemic circulation and exposure. In another recent study, Dominguez et al [75] used a peptide-specific antibody (anti-neu) to target anti-CD40-delivering PLA nanoparticles to solid tumors following intravenous administration. Although the authors demonstrated that anti-neu targeting improved the therapeutic efficacy of anti-CD40 treatments, they did not examine whether the use of targeted nanoparticles could reduce the severity or breadth of anti-CD40-induced systemic inflammation. Thus, identification of generalizable strategies to eliminate the common systemic side effects of immunotherapy agents remains an unmet need.

Here we tested the use of liposomes as nanoparticulate anchors for combinatorial immunotherapy in the setting of local therapy of established tumors, aiming to substantially alter the bio-distribution of anti-CD40 and CpG *in vivo* with the goal of blocking systemic toxicity while maintaining anti-tumor efficacy. Anti-CD40 and CpG were coupled to the surface of liposomes without loss of immunomodulatory function, via covalent conjugation or physical association to lipid anchors, and the controlled release of both ligands was demonstrated *in vitro* and *in vivo* (Figs. 1-2). Using a poorly immunogenic aggressive melanoma model in which s.c. solid tumors were allowed to establish prior to treatment, we showed that an effective anti-tumor response could be stimulated by intratumorally-injected liposome-anchored anti-CD40/CpG without inducing the signatures of systemic inflammation observed following equivalent local doses of soluble anti-CD40/CpG (Figs. 4-5). Mice that received combination liposome therapy also showed more consistent anti-tumor responses, with all mice (n=9) surviving past day 37. On the other hand, soluble immunotherapy induced a bimodal response in which 3 out of 9 mice showed minimal tumor growth for over 45 days, but the other 6 mice succumbed to tumor progression between days 28-37 (Fig. 4B). Analysis of the tissue distributions of anti-CD40 and CpG by histology (Fig. 7) and flow cytometry (Fig. 8) confirmed that liposomal delivery sequestered both ligands at the tumor site and tumor-proximal lymph node, while agents injected in soluble form were detected at significantly higher levels in the systemic circulation, particularly for anti-CD40 (Fig. 6). The maleimide-thiol reaction used here for liposomal

conjugation of anti-CD40 is generally applicable to any antibody, suggesting the potential use of this system for the delivery of additional immuno-agonists to tumors. Together, this data suggests that liposomal-anchored immunotherapies offer a promising strategy for more potent yet safe anti-tumor therapy, by providing a robust therapeutic regimen while simultaneously minimizing any indications of systemic inflammation. Further understanding of the change in therapeutic outcome obtained with liposomal delivery compared to soluble therapy (loss of a minor complete response population but gain in overall time to progression) represents a key area for further study and improvement of this approach.

A number of other studies have also described the use of biomaterial vehicles, ranging from liposomes and nanoparticles to larger microspheres and hydrogels, for the local delivery of anti-CD40, CpG, and immunomodulatory cytokines. The delivery of IL-2, IL-12, and/or GM-CSF by a variety of biomaterial carriers demonstrated significant anti-tumor effects in therapeutic challenge models, but the systemic inflammatory effects of such potent immunostimulatory treatments were not directly examined [56,59,71-72]. On the other hand, in the setting of prophylactic vaccinations (or pre-tumor challenge), Hatzifoti et al [73] found that liposomal entrapment reduced anti-CD40-induced toxicity (as measured by splenomegaly), while Bourquin et al [57] showed that s.c. injection of cationic gelatin nanoparticles carrying CpG DNA and vaccine antigens reduced systemic cytokine induction relative to soluble injections of the agonist (via decreased systemic exposure to nanoparticle-bound CpG compared to unencapsulated CpG). Conversely, De Jong et al [60] used liposomes to encapsulate CpG DNA, and surprisingly found that subcutaneous liposomal delivery dramatically increased inflammatory cytokine levels in plasma compared to subcutaneous free CpG. The disparity in systemic side effects reported in these studies might reflect differences in the stability of agonist entrapment in these various carriers, since soluble drugs or immuno-agonists released from locally-injected carriers are known to reach the systemic circulation as early as 6 hr post-injection [58,59]. These results underline the benefits of physically anchoring immuno-modulatory compounds to locally retained particle carriers, as we have proposed in the current study, compared to more commonly used encapsulation/release strategies.

A variety of leukocytic cell populations have been implicated in mediating the anti-tumor effects of anti-CD40 and CpG therapies. TLR9 expression is found predominantly in APCs such as dendritic cells, macrophages, and B cells, and the activation of any of these cells by TLR9 stimulation is known to potentiate antigen cross-priming, the production of T_H1-skewed cytokines, and the induction of potent CTL and NK-cell responses [76]. The mechanisms of anti-CD40 tumor inhibition are currently less well defined, as various studies [77-79] have implicated DCs, macrophages, B cells, or combinations thereof as the primary cells responsible for priming potent CTL or NK-cell activity [15-17,80], or T-cell independent [81] immune responses. Nevertheless, the anti-tumor efficacy of anti-CD40 and CpG therapy likely depends on their ability to stimulate APCs present in the local tumor environment, as well as APCs in the tumor-draining lymph node, where the adaptive immune response is primed. Flow cytometry analysis (Figs. 8B, E) indicated that DCs and macrophages in both locales had taken up FAM-labeled CpG and rhodamine-labeled liposomes following the i.t. injection of combination liposomes, confirming that the coupling of immuno-stimulatory ligands to liposomal carriers had not prevented them from reaching target APCs. CpG-lipid delivered via combination liposomes actually reached the tumor-draining lymph node at a higher level than soluble free CpG (Fig. 8F), although the diminished level of co-localizing rhodamine-lipid fluorescence suggests that this did not occur via the draining of intact liposomes, but rather by the draining of released CpG-lipid micelles. Whether the enhanced draining relative to free CpG was mediated by the micellar nature of the released CpG-lipid, and/or the presence of the PEG linker in the CpG-lipid conjugate, remains to be investigated. Nevertheless, this observation is consistent with the

results reported by Bourquin et al [57], in which subcutaneously injected nanoparticles increased the localization of a CpG oligonucleotide cargo to draining lymph nodes, relative to free CpG.

5. Conclusions

Recent studies in immunomodulatory therapy have achieved potent levels of anti-tumor inhibition and regression in a wide variety of pre-clinical models, but the effectiveness of this strategy in clinical treatments remains hampered by dose-limiting toxicities caused by systemic over-exposure. We have reported here the formulation and characterization of a liposomal vehicle carrying a combined dose of anti-CD40 and CpG, two highly potent anti-tumor agents. Liposomal surface coupling of these ligands retains them at a high level in the tumor and the surrounding tissue following intratumoral injection, allowing them to be presented to APCs at the tumor and the tumor-draining lymph node while restricting them from entering systemic circulation or reaching distal lymphoid organs. Future studies will be needed to elucidate the underlying mechanisms governing differences in the therapeutic outcome of liposomal vs. soluble therapy, but the results described here suggest that nanoparticle anchoring can used to block systemic toxicity while maintaining anti-tumor effects for two distinct immunostimulatory agonists.

Supplementary Material

Refer to Web version on PubMed Central for supplementary material.

Acknowledgments

This work was supported in part by the Dana-Farber/Harvard Cancer Center - MIT Bridge Project Fund. DJI is an investigator of the Howard Hughes Medical Institute. The authors would like to acknowledge the Swanson Biotechnology Center (SBC) of the Koch Institute at MIT for the use of flow cytometry and histology facilities. W. Zhang at the SBC performed the cryosectioning for histological analysis.

References

1. Whiteside TL. The tumor microenvironment and its role in promoting tumor growth. Oncogene. 2008; 27(45):5904–5912. [PubMed: 18836471]
2. Swann JB, Smyth MJ. Immune surveillance of tumors. J Clin Invest. 2007; 117(5):1137–1146. [PubMed: 17476343]
3. Kortylewski M, Swiderski P, Herrmann A, Wang L, Kowolik C, Kujawski M, et al. In vivo delivery of siRNA to immune cells by conjugation to a TLR9 agonist enhances antitumor immune responses. Nat Biotechnol. 2009; 27(10):925–932. [PubMed: 19749770]
4. Vicari AP, Chiodoni C, Vaure C, Aït-Yahia S, Dercamp C, Matsos F, et al. Reversal of tumor-induced dendritic cell paralysis by CpG immunostimulatory oligonucleotide and anti-interleukin 10 receptor antibody. J Exp Med. 2002; 196(4):541–549. [PubMed: 12186845]
5. Yang Y, Huang CT, Huang X, Pardoll DM. Persistent Toll-like receptor signals are required for reversal of regulatory T cell-mediated CD8 tolerance. Nat Immunol. 2004; 5(5):508–515. [PubMed: 15064759]
6. Houot R, Levy R. T-cell modulation combined with intratumoral CpG cures lymphoma in a mouse model without the need for chemotherapy. Blood. 2009; 113(15):3546–3552. [PubMed: 18941113]
7. Radny P, Caroli UM, Bauer J, Paul T, Schlegel C, Eigentler TK, et al. Phase II trial of intralesional therapy with interleukin-2 in soft-tissue melanoma metastases. Br J Cancer. 2003; 89(9):1620–1626. [PubMed: 14583759]
8. Jackaman C, Lew AM, Zhan Y, Allan JE, Koloska B, Graham PT, et al. Deliberately provoking local inflammation drives tumors to become their own protective vaccine site. Int Immunol. 2008; 20(11):1467–1479. [PubMed: 18824504]

9. Curran MA, Montalvo W, Yagita H, Allison JP. PD-1 and CTLA-4 combination blockade expands infiltrating T cells and reduces regulatory T and myeloid cells within B16 melanoma tumors. Proc Natl Acad Sci USA. 2010; 107(9):4275–4280. [PubMed: 20160101]

10. Pardoll DM. Paracrine cytokine adjuvants in cancer immunotherapy. Annu Rev Immunol. 1995; 13:399–415. [PubMed: 7612229]

11. Elgueta R, Benson MJ, de Vries VC, Wasiuk A, Guo Y, Noelle RJ. Molecular mechanism and function of CD40/CD40L engagement in the immune system. Immunol Rev. 2009; 229(1):152–172. [PubMed: 19426221]

12. Carson WE, Dierksheide JE, Jabbour S, Anghelina M, Bouchard P, Ku G, et al. Coadministration of interleukin-18 and interleukin-12 induces a fatal inflammatory response in mice: critical role of natural killer cell interferon-gamma production and STAT-mediated signal transduction. Blood. 2000; 96(4):1465–1473. [PubMed: 10942393]

13. Phan GQ, Yang JC, Sherry RM, Hwu P, Topalian SL, Schwartzentruber DJ, et al. Cancer regression and autoimmunity induced by cytotoxic T lymphocyte-associated antigen 4 blockade in patients with metastatic melanoma. Proc Natl Acad Sci USA. 2003; 100(14):8372–8377. [PubMed: 12826605]

14. Diehl L, den Boer AT, Schoenberger SP, van der Voort EI, Schumacher TN, Melief CJ, et al. CD40 activation in vivo overcomes peptide-induced peripheral cytotoxic T-lymphocyte tolerance and augments anti-tumor vaccine efficacy. Nat Med. 1999; 5(7):774–779. [PubMed: 10395322]

15. French RR, Chan HT, Tutt AL, Glennie MJ. CD40 antibody evokes a cytotoxic T-cell response that eradicates lymphoma and bypasses T-cell help. Nat Med. 1999; 5(5):548–553. [PubMed: 10229232]

16. Sotomayor EM, Borrello I, Tubb E, Rattis FM, Bien H, Lu Z, et al. Conversion of tumor-specific CD4+ T-cell tolerance to T-cell priming through in vivo ligation of CD40. Nat Med. 1999; 5(7): 780–787. [PubMed: 10395323]

17. Tutt AL, O'Brien L, Hussain A, Crowther GR, French RR, Glennie MJ. T cell immunity to lymphoma following treatment with anti-CD40 monoclonal antibody. J Immunol. 2002; 168(6): 2720–2728. [PubMed: 11884438]

18. van Mierlo GJ, den Boer AT, Medema JP, van der Voort EI, Fransen MF, Offringa R, et al. CD40 stimulation leads to effective therapy of CD40(-) tumors through induction of strong systemic cytotoxic T lymphocyte immunity. Proc Natl Acad Sci USA. 2002; 99(8):5561–5566. [PubMed: 11929985]

19. Todryk SM, Tutt AL, Green MH, Smallwood JA, Halanek N, Dalgleish AG, et al. CD40 ligation for immunotherapy of solid tumours. J Immunol Methods. 2001; 248(1-2):139–147. [PubMed: 11223075]

20. Nowak AK, Robinson BW, Lake RA. Synergy between chemotherapy and immunotherapy in the treatment of established murine solid tumors. Cancer Res. 2003; 63(15):4490–4496. [PubMed: 12907622]

21. Murphy WJ, Welniak L, Back T, Hixon J, Subleski J, Seki N, et al. Synergistic anti-tumor responses after administration of agonistic antibodies to CD40 and IL-2: coordination of dendritic and CD8+ cell responses. J Immunol. 2003; 170(5):2727–2733. [PubMed: 12594303]

22. Hamzah J, Nelson D, Moldenhauer G, Arnold B, Hammerling GJ, Ganss R. Vascular targeting of anti-CD40 antibodies and IL-2 into autochthonous tumors enhances immunotherapy in mice. J Clin Invest. 2008; 118(5):1691–1699. [PubMed: 18398504]

23. Vonderheide RH, Flaherty KT, Khalil M, Stumacher MS, Bajor DL, Hutnick NA, et al. Clinical activity and immune modulation in cancer patients treated with CP-870,893, a novel CD40 agonist monoclonal antibody. J Clin Oncol. 2007; 25(7):876–883. [PubMed: 17327609]

24. Hussein M, Berenson JR, Niesvizky R, Munshi N, Matous J, Sobecks R, et al. A phase I multidose study of dacetuzumab (SGN-40; humanized anti-CD40 monoclonal antibody) in patients with multiple myeloma. Haematologica. 2010; 95(5):845–848. [PubMed: 20133895]

25. Advani R, Forero-Torres A, Furman RR, Rosenblatt JD, Younes A, Ren H, et al. Phase I study of the humanized anti-CD40 monoclonal antibody dacetuzumab in refractory or recurrent non-Hodgkin's lymphoma. J Clin Oncol. 2009; 27(26):4371–4377. [PubMed: 19636010]

26. Ruter J, Antonia SJ, Burris HA, Huhn RD, Vonderheide RH. Immune modulation with weekly dosing of an agonist CD40 antibody in a phase I study of patients with advanced solid tumors. Cancer Biol Ther. 2010; 10(10):983–993. [PubMed: 20855968]
27. Kimura K, Moriwaki H, Nagaki M, Saio M, Nakamoto Y, Naito M, et al. Pathogenic role of B cells in anti-CD40-induced necroinflammatory liver disease. Am J Pathol. 2006; 168(3):786–795. [PubMed: 16507894]
28. Wiley JA, Geha R, Harmsen AG. Exogenous CD40 ligand induces a pulmonary inflammation response. J Immunol. 1997; 158(6):2932–2938. [PubMed: 9058832]
29. Gendelman M, Halligan N, Komorowski R, Logan B, Murphy WJ, Blazar BR, et al. Alpha phenyl-tert-butyl nitrone (PBN) protects syngeneic marrow transplant recipients from the lethal cytokine syndrome occurring after agonistic CD40 antibody administration. Blood. 2005; 105(1):428–431. [PubMed: 15331451]
30. Hixon JA, Anver MR, Blazar BR, Panoskaltsis-Mortari A, Wiltrout RH, Murphy WJ. Administration of either anti-CD40 or interleukin-12 following lethal total body irradiation induces acute lethal toxicity affecting the gut. Biol Blood Marrow Transplant. 2002; 8(6):316–325. [PubMed: 12108917]
31. Berner V, Liu H, Zhou Q, Alderson KL, Sun K, Weiss JM, et al. IFN-gamma mediates CD4+ T-cell loss and impairs secondary antitumor responses after successful initial immunotherapy. Nat Med. 2007; 13(3):354–360. [PubMed: 17334371]
32. Bartholdy C, Kauffmann SO, Christensen JP, Thomsen AR. Agonistic anti-CD40 antibody profoundly suppresses the immune response to infection with lymphocytic choriomeningitis virus. J Immunol. 2007; 178(3):1662–1670. [PubMed: 17237416]
33. Krieg AM. Toll-like receptor 9 (TLR9) agonists in the treatment of cancer. Oncogene. 2008; 27(2): 161–167. [PubMed: 18176597]
34. Lonsdorf AS, Kuekrek H, Stern BV, Boehm BO, Lehmann PV, Tary-Lehmann M. Intratumor CpG-oligodeoxynucleotide injection induces protective antitumor T cell immunity. J Immunol. 2003; 171(8):3941–3946. [PubMed: 14530311]
35. Baines J, Celis E. Immune-mediated tumor regression induced by CpG-containing oligodeoxynucleotides. Clin Cancer Res. 2003; 9(7):2693–2700. [PubMed: 12855649]
36. Heckelsmiller K, Rall K, Beck S, Schlamp A, Seiderer J, Jahrsdorfer B, et al. Peritumoral CpG DNA elicits a coordinated response of CD8 T cells and innate effectors to cure established tumors in a murine colon carcinoma model. J Immunol. 2002; 169(7):3892–3899. [PubMed: 12244187]
37. Stone GW, Barzee S, Snarsky V, Santucci C, Tran B, Langer R, et al. Nanoparticle-delivered multimeric soluble CD40L DNA combined with Toll-Like Receptor agonists as a treatment for melanoma. PLoS One. 2009; 4(10):e7334. [PubMed: 19812695]
38. Buhtoiarov IN, Lum HD, Berke G, Sondel PM, Rakhmilevich AL. Synergistic activation of macrophages via CD40 and TLR9 results in T cell independent antitumor effects. J Immunol. 2006; 176(1):309–318. [PubMed: 16365423]
39. Ahonen CL, Wasiuk A, Fuse S, Turk MJ, Ernstoff MS, Suriawinata AA, et al. Enhanced efficacy and reduced toxicity of multifactorial adjuvants compared with unitary adjuvants as cancer vaccines. Blood. 2008; 111(6):3116–3125. [PubMed: 18202224]
40. Scarlett UK, Cubillos-Ruiz JR, Nesbeth YC, Martinez DG, Engle X, Gewirtz AT, et al. In situ stimulation of CD40 and Toll-like receptor 3 transforms ovarian cancer-infiltrating dendritic cells from immunosuppressive to immunostimulatory cells. Cancer Res. 2009; 69(18):7329–7337. [PubMed: 19738057]
41. Heikenwalder M, Polymenidou M, Junt T, Sigurdson C, Wagner H, Akira S, et al. Lymphoid follicle destruction and immunosuppression after repeated CpG oligodeoxynucleotide administration. Nat Med. 2004; 10(2):187–192. [PubMed: 14745443]
42. Mellor AL, Baban B, Chandler PR, Manlapat A, Kahler DJ, Munn DH. Cutting edge: CpG oligonucleotides induce splenic CD19+ dendritic cells to acquire potent indoleamine 2,3-dioxygenase-dependent T cell regulatory functions via IFN Type 1 signaling. J Immunol. 2005; 175(9):5601–5605. [PubMed: 16237046]

43. Wingender G, Garbi N, Schumak B, Jungerkes F, Endl E, von Bubnoff D, et al. Systemic application of CpG-rich DNA suppresses adaptive T cell immunity via induction of IDO. Eur J Immunol. 2006; 36(1):12–20. [PubMed: 16323249]
44. Gimbel MI, Delman KA, Zager JS. Therapy for unresectable recurrent and in-transit extremity melanoma. Cancer Control. 2008; 15(3):225–232. [PubMed: 18596674]
45. Mundt AJ, Vijayakumar S, Nemunaitis J, Sandler A, Schwartz H, Hanna N, et al. A Phase I trial of TNFerade biologic in patients with soft tissue sarcoma in the extremities. Clin Cancer Res. 2004; 10(17):5747–5753. [PubMed: 15355902]
46. Grasso M, Torelli F, Scannapieco G, Franzoso F, Lania C. Neoadiuvant Treatment With Intravesical Interleukin-2 for Recurrent Superficial Transitional Bladder Carcinoma Ta- T1/G1-2. J Immunother. 2001; 24(2):184–187.
47. Den Otter W, Jacobs JJ, Battermann JJ, Hordijk GJ, Krastev Z, Moiseeva EV, et al. Local therapy of cancer with free IL-2. Cancer Immunol Immunother. 2008; 57(7):931–950. [PubMed: 18256831]
48. Johnson EE, Lum HD, Rakhmilevich AL, Schmidt BE, Furlong M, Buhtoiarov IN, et al. Intratumoral immunocytokine treatment results in enhanced antitumor effects. Cancer Immunol Immunother. 2008; 57:1891–1902. [PubMed: 18438664]
49. Simmons AD, Moskalenko M, Creson J, Fang J, Yi S, VanRoey MJ, et al. Local secretion of anti-CTLA-4 enhances the therapeutic efficacy of a cancer immunotherapy with reduced evidence of systemic autoimmunity. Cancer Immunol Immunother. 2008; 57(8):1263–1270. [PubMed: 18236040]
50. Broomfield SA, van der Most RG, Prosser AC, Mahendran S, Tovey MG, Smyth MJ, et al. Locally administered TLR7 agonists drive systemic antitumor immune responses that are enhanced by anti-CD40 immunotherapy. J Immunol. 2009; 182(9):5217–5224. [PubMed: 19380767]
51. Galili U, Wigglesworth K, Abdel-Motal UM. Intratumoral injection of alpha-gal glycolipids induces xenograft-like destruction and conversion of lesions into endogenous vaccines. J Immunol. 2007; 178(7):4676–4687. [PubMed: 17372027]
52. Broderick L, Yokota SJ, Reineke J, Mathiowitz E, Stewart CC, Barcos M, et al. Human CD4+ effector memory T cells persisting in the microenvironment of lung cancer xenografts are activated by local delivery of IL-12 to proliferate, produce IFN-g, and eradicate tumor cells. J Immunol. 2005; 174:898–906. [PubMed: 15634912]
53. Brody JD, Ai WZ, Czerwinski DK, Torchia JA, Levy M, Advani RH, et al. In situ vaccination with a TLR9 agonist induces systemic lymphoma regression: a phase I/II study. J Clin Oncol. 2010; 28(28):4324–4332. [PubMed: 20697067]
54. Eton O, Rosenblum MG, Legha SS, Zhang W, Jo East M, Bedikian A, et al. Phase I trial of subcutaneous recombinant human Interleukin-2 in patients with metastatic melanoma. Cancer. 2002; 95(1):127–134. [PubMed: 12115326]
55. Portielje JEA, Kruit WHJ, Schuler M, Beck J, Lamers CHJ, Stoter G, et al. Phase I study of subcutaneously administered recombinant human interleukin-12 in patients with advanced renal cell cancer. Clin Cancer Res. 1999; 5:3983–3989. [PubMed: 10632329]
56. Hanes J, Sills A, Zhao Z, Suh KW, Tyler B, DiMeco F, et al. Controlled local delivery of interleukin-2 by biodegradable polymers protects animals from experimental brain tumors and liver tumors. Pharm Res. 2001; 18(7):899–906. [PubMed: 11496947]
57. Bourquin C, Anz D, Zwiorek K, Lanz AL, Fuchs S, Weigel S, et al. Targeting CpG oligonucleotides to the lymph node by nanoparticles elicits efficient antitumoral immunity. J Immunol. 2008; 181(5):2990–2998. [PubMed: 18713969]
58. Hori Y, Stern PJ, Hynes RO, Irvine DJ. Engulfing tumors with synthetic extracellular matrices for cancer immunotherapy. Biomaterials. 2009; 30(35):6757–6767. [PubMed: 19766305]
59. Hill HC, Conway TF Jr, Sabel MS, Jong YS, Mathiowitz E, Bankert RB, et al. Cancer immunotherapy with interleukin 12 and granulocyte-macrophage colony-stimulating factor-encapsulated microspheres: coinduction of innate and adaptive antitumor immunity and cure of disseminated disease. Cancer Res. 2002; 62(24):7254–7263. [PubMed: 12499267]
60. de Jong S, Chikh G, Sekirov L, Raney S, Semple S, Klimuk S, et al. Encapsulation in liposomal nanoparticles enhances the immunostimulatory, adjuvant and anti-tumor activity of

subcutaneously administered CpG ODN. Cancer Immunol Immunother. 2007; 56(8):1251–1264. [PubMed: 17242927]

61. Van Herpen CM, Huijbens R, Looman M, De Vries J, Marres H, Van De Ven J, et al. Pharmacokinetics and immunological aspects of a phase Ib study with intratumoral administration of recombinant human interleukin-12 in patients with head and neck squamous cell carcinoma: a decrease of T-bet in peripheral blood mononuclear cells. Clin Cancer Res. 2003; 9(8):2950–2956. [PubMed: 12912941]
62. Lienard D, Ewalenko P, Delmotte JJ, Renard N, Lejeune FJ. High-dose recombinant tumor necrosis factor alpha in combination with interferon gamma and melphalan in isolation perfusion of the limbs for melanoma and sarcoma. J Clin Oncol. 1992; 10(1):52–60. [PubMed: 1727926]
63. Bartlett DL, Libutti SK, Figg WD, Fraker DL, Alexander HR. Isolated hepatic perfusion for unresectable hepatic metastases from colorectal cancer. Surgery. 2001; 129(2):176–187. [PubMed: 11174711]
64. Liu H, Zhu Z, Kang H, Wu Y, Sefan K, Tan W. DNA-based micelles: synthesis, micellar properties and size-dependent cell permeability. Chemistry. 2010; 16(12):3791–3797. [PubMed: 20162643]
65. Allen TM, Sapra P, Moase E. Use of the post-insertion method for the formation of ligand-coupled liposomes. Cell Mol Biol Lett. 2002; 7(3):889–894. [PubMed: 12378272]
66. Ruegg UT, Rudinger J. Reductive cleavage of cystine disulfides with tributylphosphine. Methods Enzymol. 1977; 47:111–116. [PubMed: 927167]
67. Fattori E, Cappelletti M, Costa P, Sellitto C, Cantoni L, Carelli M, et al. Defective inflammatory response in interleukin 6-deficient mice. J Exp Med. 1994; 180(4):1243–1250. [PubMed: 7931061]
68. Strassmann G, Fong M, Windsor S, Neta R. The role of interleukin-6 in lipopolysaccharide-induced weight loss, hypoglycemia and fibrinogen production, in vivo. Cytokine. 1993; 5(4):285–290. [PubMed: 8260592]
69. Krieg AM, Stein CA. Phosphorothioate oligodeoxynucleotides: antisense or anti-protein? Antisense Res Dev. 1995; 5(4):241. [PubMed: 8746772]
70. Rutz M, Metzger J, Gellert T, Luppa P, Lipford GB, Wagner H, et al. Toll-like receptor 9 binds single-stranded CpG-DNA in a sequence- and pH-dependent manner. Eur J Immunol. 2004; 34:2541–2550. [PubMed: 15307186]
71. Neville ME, Robb RJ, Popescu MC. In situ vaccination against a non-immunogenic tumour using intratumoural injections of liposomal interleukin-2. Cytokine. 2001; 16(6):239–250. [PubMed: 11884028]
72. Sabel MS, Arora A, Su G, Mathiowitz E, Reineke JJ, Chang AE. Synergistic effect of intratumoral IL-12 and TNF-a microspheres: systemic anti-tumor immunity is mediated by both CD8+ CTL and NK cells. Surgery. 2007; 142(5):749–760. [PubMed: 17981196]
73. Hatzifoti C, Bacon A, Marriott H, Laing P, Heath AW. Liposomal co-entrapment of CD40mAb induces enhanced IgG responses against bacterial polysaccharide and protein. PLoS One. 2008; 3(6):e2368. [PubMed: 18523585]
74. Hamzah J, Altin JG, Herringson T, Parish CR, Hammerling GJ, O'Donoghue H, et al. Targeted liposomal delivery of TLR9 ligands activates spontaneous antitumor immunity in an autochthonous cancer model. J Immunol. 2009; 183(2):1091–1098. [PubMed: 19561111]
75. Dominguez AL, Lustgarten J. Targeting the tumor microenvironment with anti-neu/anti- CD40 conjugated nanoparticles for the induction of antitumor immune responses. Vaccine. 2010; 28(5): 1383–1390. [PubMed: 19931385]
76. Klinman DM. Immunotherapeutic uses of CpG oligodeoxynucleotides. Nat Rev Immunol. 2004; 4(4):249–258. [PubMed: 15057783]
77. van Mierlo GJ, Boonman ZF, Dumortier HM, den Boer AT, Fransen MF, Nouta J, et al. Activation of dendritic cells that cross-present tumor-derived antigen licenses CD8+ CTL to cause tumor eradication. J Immunol. 2004; 173(11):6753–6759. [PubMed: 15557168]
78. Oflazoglu E, Stone IJ, Brown L, Gordon KA, van Rooijen N, Jonas M, et al. Macrophages and Fc-receptor interactions contribute to the antitumour activities of the anti-CD40 antibody SGN-40. Br J Cancer. 2009; 100(1):113–117. [PubMed: 19066610]

79. Jackaman C, Cornwall S, Graham PT, Nelson DJ. CD40-activated B cells contribute to mesothelioma tumor regression. Immunol Cell Biol. 2010 epub ahead of print.

80. Stumbles PA, Himbeck R, Frelinger JA, Collins EJ, Lake RA, Robinson BW. Cutting edge: tumor-specific CTL are constitutively cross-armed in draining lymph nodes and transiently disseminate to mediate tumor regression following systemic CD40 activation. J Immunol. 2004; 173(10): 5923–5928. [PubMed: 15528325]

81. Rakhmilevich AL, Buhtoiarov IN, Malkovsky M, Sondel PM. CD40 ligation in vivo can induce T cell independent antitumor effects even against immunogenic tumors. Cancer Immunol Immunother. 2008; 57(8):1151–1160. [PubMed: 18214476]

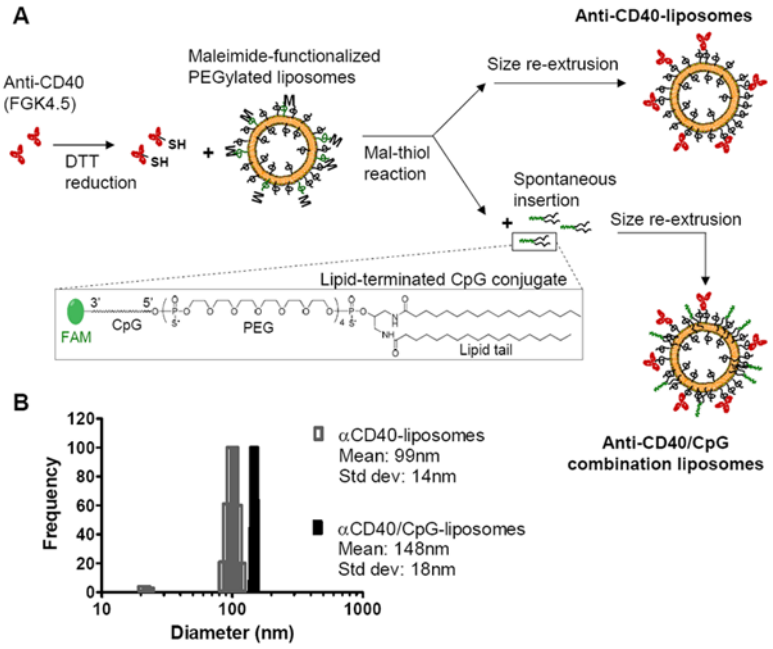

Figure 1.

Synthesis of PEGylated liposomes bearing lipid-anchored anti-CD40 and CpG oligonucleotides. (A) Schematic illustration of the surface coupling of anti-CD40 to PEGylated liposomes via maleimide-thiol reaction, followed by the insertion of the CpG-lipid conjugate into the surface of antibody-coupled liposomes. The structure of the synthetic CpG oligonucleotide-lipid conjugate is shown, including a polyethylene glycol (PEG) spacer and a fluorescein label attached at the 3' end. (B) Size distributions of anti-CD40 liposomes and anti-CD40/CpG liposomes following membrane re-extrusion, as measured by dynamic light scattering.

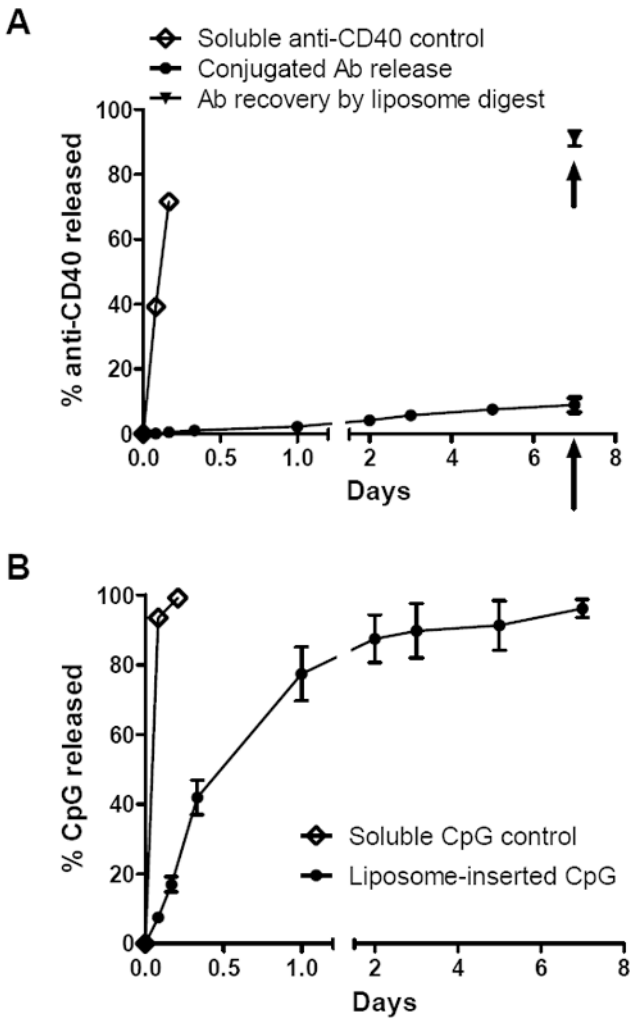

Figure 2.

Controlled release of anti-CD40 and CpG from combination liposomes (filled symbols) by dialysis against serum-containing PBS *in vitro*, compared to the dialysis of freely soluble immuno-agonists (open symbols). (A) Release of conjugated anti-CD40 from combination liposomes, over 7 days of dialysis. On day 7, liposomes were disrupted with Tween 20 (arrow) and the amount of recovered anti-CD40 was measured. (B) Release of inserted CpG-lipid from combination liposomes, reaching a plateau after ~2 days.

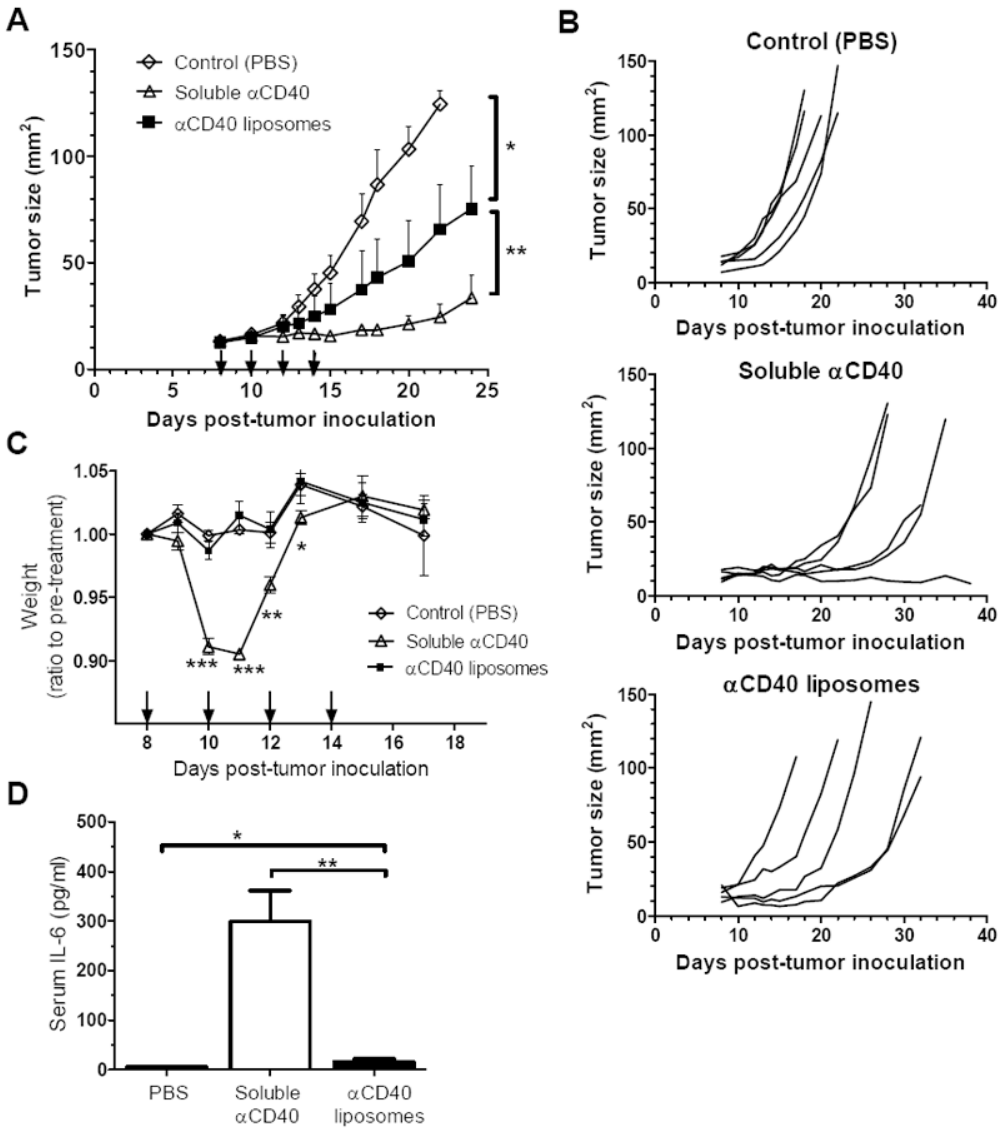

Figure 3.

B16 melanoma therapy using locally-injected soluble anti-CD40 or liposome-anchored anti-CD40. (A) Average tumor growth curves from a representative experiment (n = 5 mice/group). Arrows indicate 4 intra-tumoral injections (days 8,10,12,14 following tumor cell inoculation) at an equivalent dose of 40 μg anti-CD40 per injection. P-values were determined by paired t-tests: *p=0.01, **p=0.005. (B) Individual tumor growth curves of subcutaneously implanted B16 tumors, treated with local injections of PBS, soluble anti-CD40, or anti-CD40-liposomes, according to the dose regimen described in (A). (C) Transient weight loss as a gross indication of the systemic side effects caused by local soluble anti-CD40 therapy, but not anti-CD40-liposome therapy (injections denoted by arrows). Statistically significant differences in comparison to PBS controls were determined by unpaired t-test at each timepoint: *p=0.04, **p=0.004, ***p<0.0001. (D) Circulating serum levels of the inflammatory cytokine IL-6 at 24 hours following the first dose of intra-tumoral soluble anti-CD40 therapy or anti-CD40-liposome therapy. P-values were determined by unpaired t-test: *p=0.11(N.S.), **p=0.002.

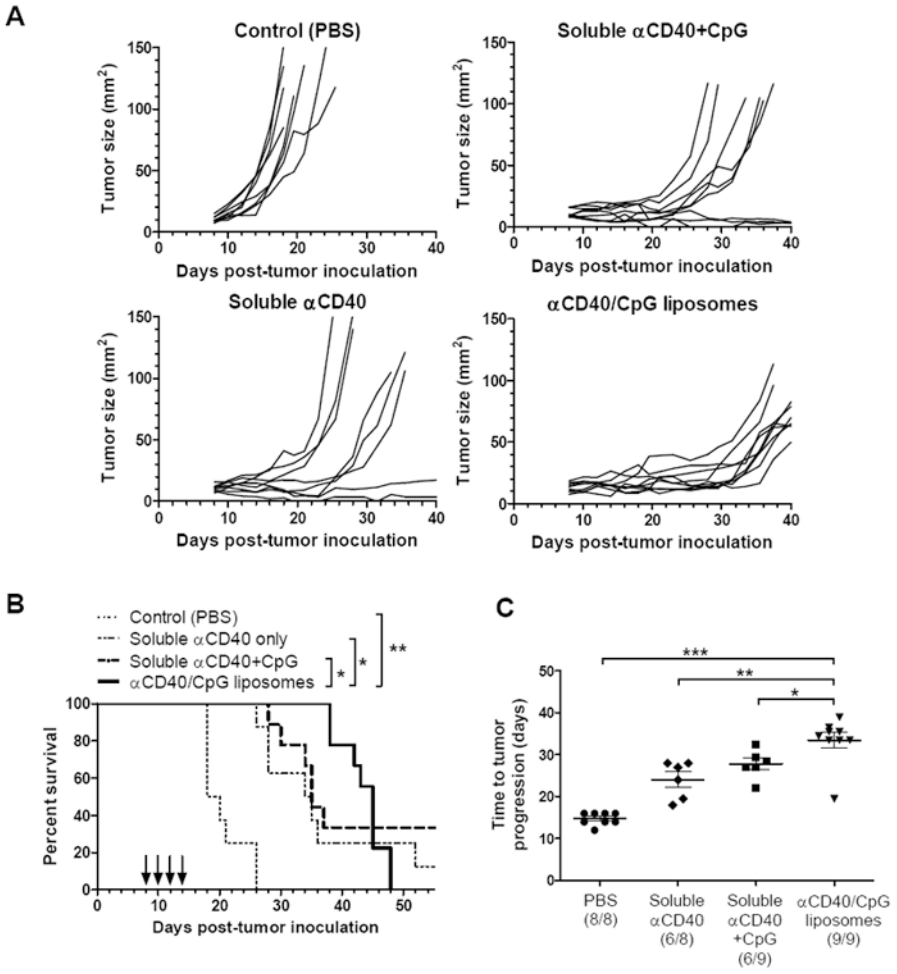

Figure 4.

Treatment of B16 melanoma via soluble anti-CD40 + CpG vs. liposome-anchored anti-CD40/CpG. (A) Individual tumor growth curves (n=8 or 9 mice/group), combined from two independent experiments. Mice were given 4 intra-tumoral injections (days 8,10,12,14) of PBS, soluble anti-CD40, soluble anti-CD40+CpG, or anti-CD40/CpG liposomes, at equivalent doses of 40 μg anti-CD40 and 20 μg CpG per injection. (B) Kaplan-Meier survival curves of B16 tumor-bearing mice following the treatment regimen described in (A). Mice were euthanized when tumor burden exceeded 100mm^2. P-values were determined by Log-rank test: *p=N.S., **p<0.0001. (C) Time to tumor progression for partial responders to therapy, defined as the day at which tumor burden reached 3x the initial tumor size at the start of therapy (dosing regimen as described in (A)). Parentheses indicate the fraction of mice from each group that were accounted in this analysis (complete responders in soluble anti-C40-receiving groups were omitted). P-values were determined by unpaired t-test: *p=0.04, **p=0.004, ***p<0.0001.

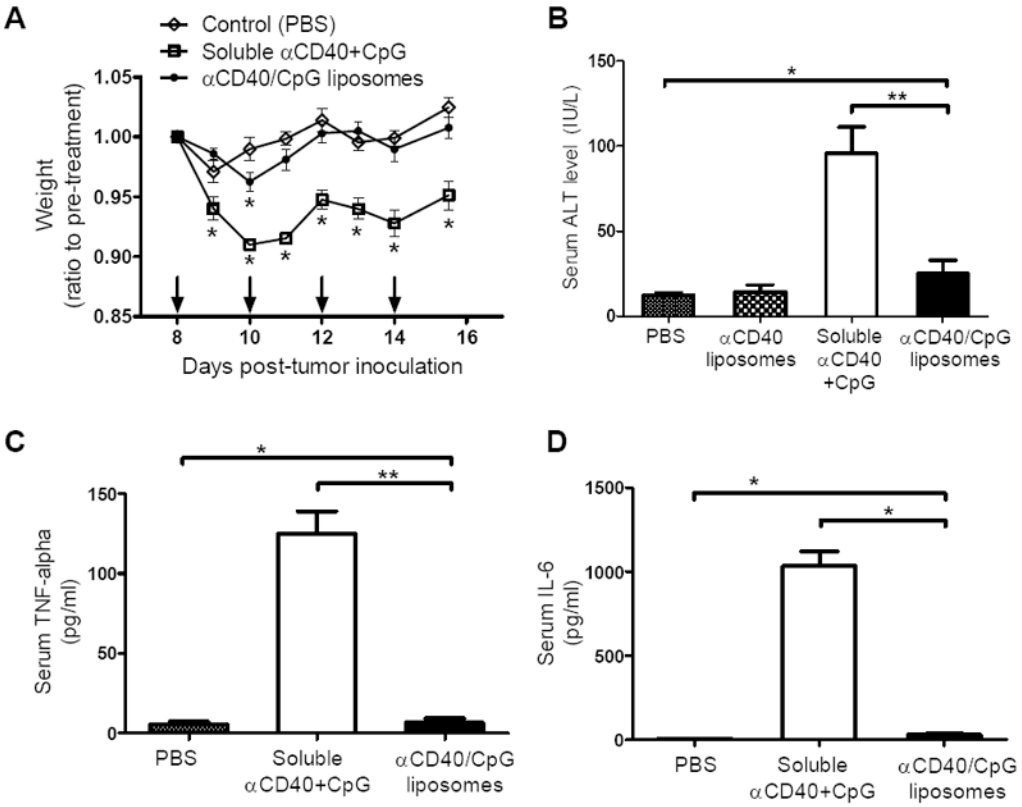

Figure 5.

Systemic toxicity following soluble vs. liposomal anti-CD40/CpG immunotherapy. (A) Weight loss following intratumoral injections of PBS, soluble anti-CD40+CpG, or anti-CD40/CpG liposomes, following an identical dosing regimen as described in Figure 4. Statistically significant differences in comparison to PBS controls were determined by unpaired t-test at each timepoint: *p≤0.04. (B) Serum circulating levels of hepatic ALT enzyme at 24hr following the first dose of soluble or liposomal immunotherapy. P-values determined by unpaired t-test: *p=0.07(N.S.), **p=0.004. (C) Serum circulating levels of the inflammatory cytokine TNF-α, at 24 hr following the first dose of soluble or liposomal anti-CD40/CpG; *p=0.8(N.S.), **p<0.0001. (D) Serum circulating levels of the inflammatory cytokine IL-6, at 24hr following the first dose of therapy; *p<0.0001.

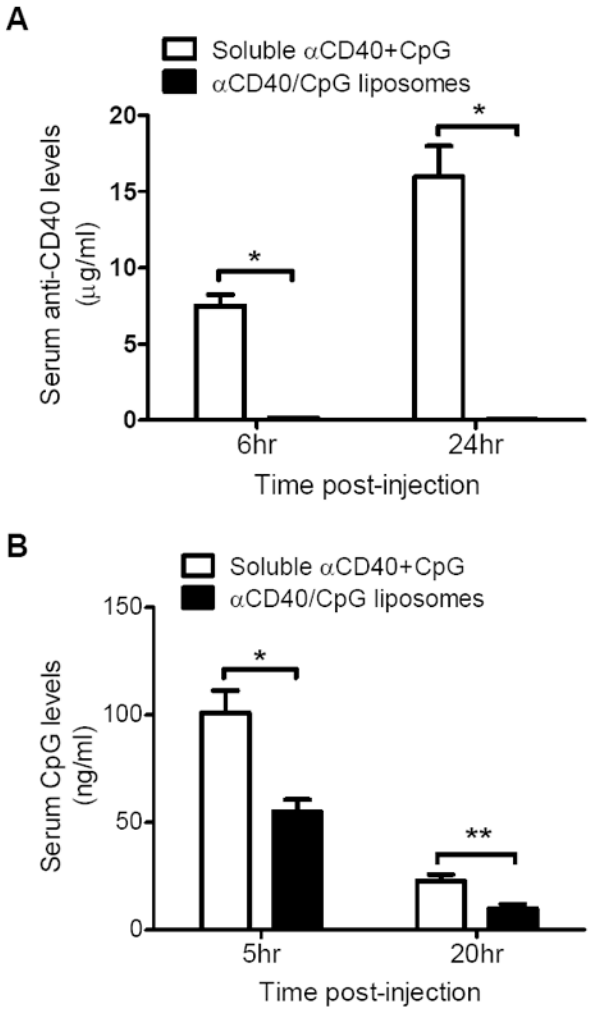

Figure 6.

Systemic exposure to anti-CD40 and CpG following soluble or liposomal local immunotherapy. (A) Serum levels of anti-CD40 at 6 hr and 24 hr after an intratumoral injection of soluble or combination liposome therapy. P-values determined by unpaired t-test: *$p<0.0001$. (B) Serum levels of CpG at 5 hr and 20 hr after an intratumoral injection of soluble or liposomal combination therapy. P-values determined by unpaired t-test: *$p=0.0008$, **$p=0.002$.

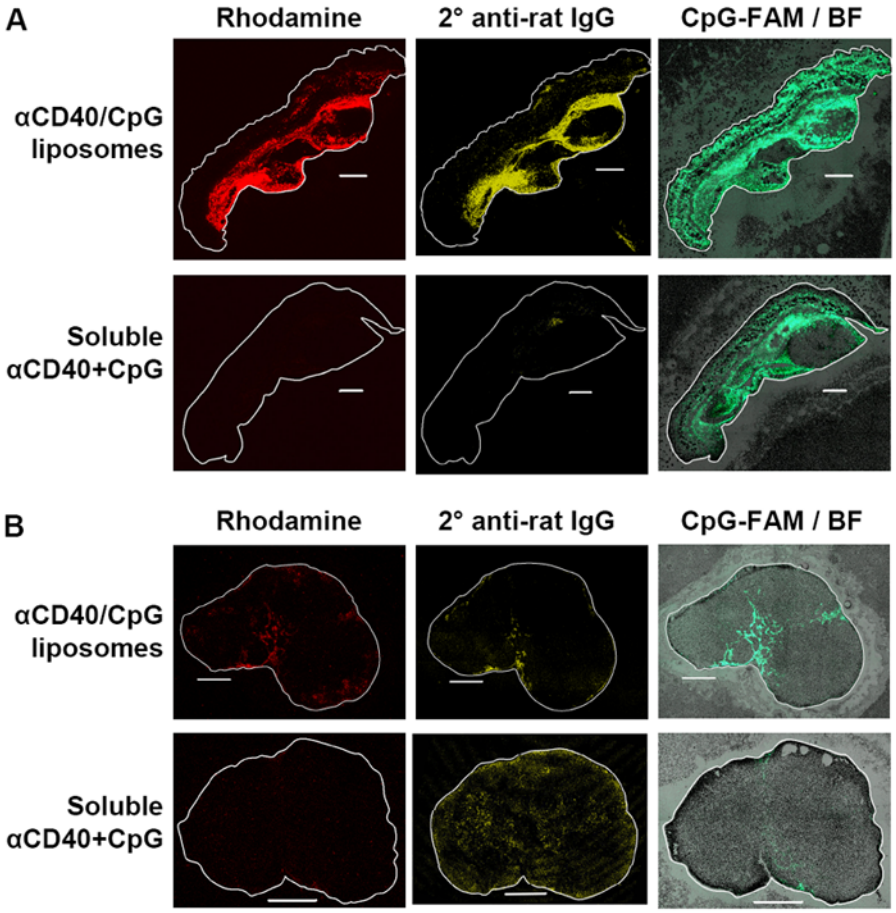

Figure 7.

Histological analysis of anti-CD40 and CpG biodistributions following local immunotherapy. Immunohistochemical staining of frozen tissue sections showing fluorescent rhodamine-labeled liposomes (left panels, red); anti-CD40 (middle panels, yellow); and CpG (right panels, green overlaid with brightfield image). Edges of the tissue sections are outlined in white; scale bars denote 500 μm. (A) Representative cryosections of subcutaneous tumors and the surrounding tissue, taken at 48 hr following a local injection of soluble or liposomal anti-CD40/CpG. (B) Representative cryosections of tumor-proximal lymph nodes, taken at 24 hr following an intra-tumoral injection of soluble or liposomal anti-CD40/CpG.

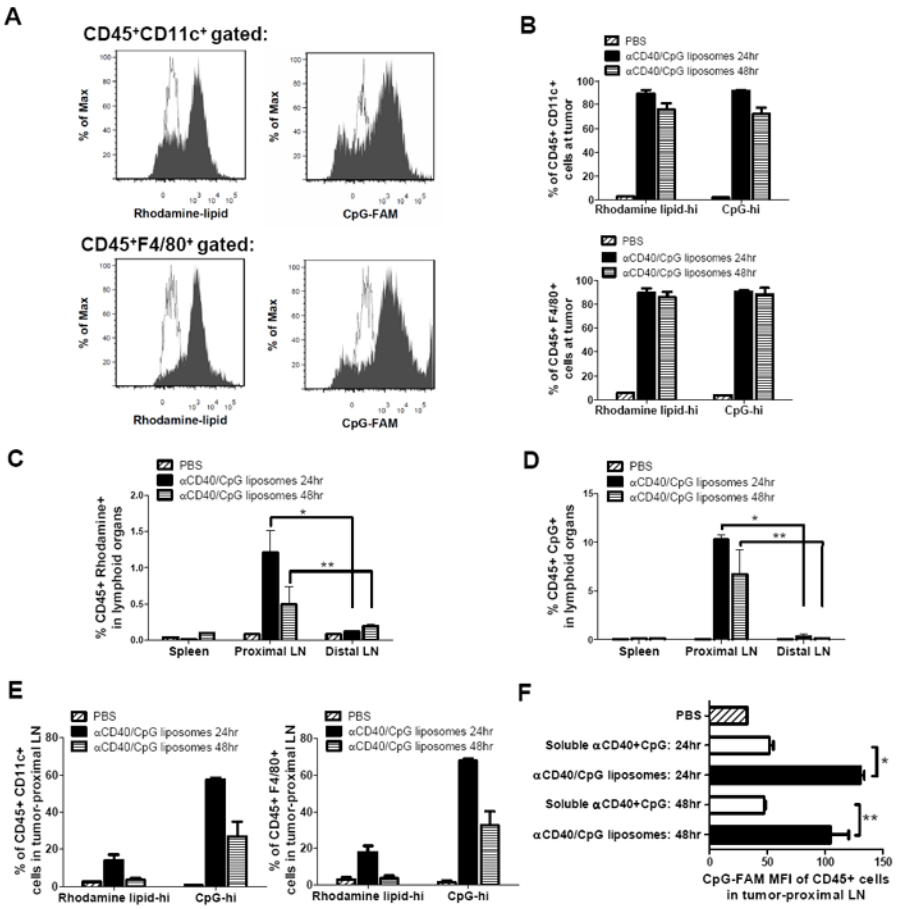

Figure 8.

Flow cytometry analysis of excised tumors and proximal or distal lymphoid organs following local immunotherapy. (A) Representative histograms of excised tumor tissues at 48 hr following a single intratumoral injection of anti-CD40/CpG liposomes, showing the uptake of rhodamine-labeled liposomes (left) and FAM-labeled CpG (right) by the majority of dendritic cells (top, CD45+CD11c+ staining) or macrophages (bottom, CD45+F4/80+ staining). Filled histograms = liposomal therapy; open histograms = background fluorescence from PBS-treated controls. (B) Bar graph summary of the flow cytometry analysis depicted in (A), showing the percentage of dendritic cells (top) or macrophages (bottom) positive for rhodamine-liposomes or FAM-CpG in excised tumor tissues. (C) Flow cytometry analysis of distal and tumor-proximal lymphoid organs following a single dose of liposomal anti-CD40/CpG therapy, indicating preferential drainage of rhodamine-labeled liposomes to the tumor-proximal lymph node, with minimal leakage to distal lymph nodes or the spleen. P-values determined by unpaired t-test: *p=0.03, **p=0.14(N.S.). (D) Flow cytometry analysis showing preferential local drainage of FAM-labeled CpG, analogous to part (C); *p<0.0001, **p=0.03. (E) Co-staining of rhodamine-labeled liposomes or FAM-labeled CpG with dendritic cells (left, CD45+CD11c+) and macrophages (right, $CD45^+F4/80^+$) in the tumor-proximal lymph node, following a single intra-tumoral liposomal injection. (F) Mean fluorescent intensity (MFI) of FAM-labeled CpG in $CD45^+$ leukocytes in the tumor-proximal lymph node following intra-tumoral soluble or liposomal anti-CD40/CpG treatment. The level of CpG in the draining lymph node is enhanced by liposomal delivery of the CpG-lipid conjugate; *p<0.0001, **p=0.02.